

Detecting Eyelash and Reflection for Accurate Iris Segmentation

Wai-Kin Kong and David Zhang

Biometrics Research Centre
Department of Computing, The Hong Kong Polytechnic University
Kowloon, Hong Kong

Corresponding author:

Prof. David Zhang

Biometrics Research Centre

Department of Computing

Hong Kong Polytechnic University

Hung Hom, Kowloon, Hong Kong

Phone: (852) 2766-7271

Fax: (852) 2774-0842

E-mail: csdzhang@comp.polyu.edu.hk

Abstract — Accurate iris segmentation is presented in this paper, which is composed of two parts, reflection detection and eyelash detection. Eyelashes are classified into two categories, separable and multiple. An edge detector is applied to detect separable eyelashes and intensity variances are used to recognize multiple eyelashes. Reflection is also divided into two types, strong and weak. A threshold and statistical test are proposed to recognize the strong and weak reflection, respectively. We have developed an iris recognition approach for testing the effectiveness of the proposed segmentation method. The results show that the proposed method can reduce recognition error for the iris recognition approach.

Key Terms — Segmentation, eyelash, reflection, iris recognition, biometric

1. Introduction

Accurate iris segmentation is an important step for automatic iris recognition and iridology [1-5]. In the previous iris segmentation approaches [1-3], the inner and outer boundaries of an iris can be taken as two non-centric circles and the upper and lower eyelids are modeled by two parabolas. Hough transform and other curves fitting techniques are capable of effectively determining the parameters of the circles and parabolas [8-9]. Fig. 1 shows a segmented result of the previous approaches. However, eyelashes and reflection are neglected by the previous approaches. For automatic iris recognition, if eyelashes or reflection pixels are considered as iris pixels, the performance of iris recognition systems is degraded; as a result, it motivates us to propose a method to detect eyelashes and reflection.

This paper is organized as follows: Section 2 and Section 3 discuss our eyelash and reflection detection models, respectively. An iris recognition approach is described in Section 4,

which is used to test the proposed segmentation model. Experimental results are given in Section 5. Finally, some conclusion is presented in Section 6.

2. Eyelash Segmentation

Two classes of eyelashes are defined in our eyelash detection model, separable and multiple eyelashes. Separable eyelashes are defined as the eyelashes that can be distinguished from other eyelashes and multiple eyelashes are the eyelashes that overlap in a small area. Fig. 1 illustrates the two classes of eyelashes.

2.1. Separable Eyelashes

By the definition of separable eyelashes, they can be distinguished from other eyelashes; thus, the pixels around separable eyelash should not belong to other eyelashes. In fact, most of pixels around separable eyelashes are iris pixels. Because of the intensity difference between iris pixels and eyelashes pixels, a separable eyelash can be regarded as an edge in an image. Fig. 2 shows a cross section of a separable eyelash gray level and part of iris around it. Based on this property, a real part of Gabor filter is proposed to detect separable eyelashes, which, in the spatial domain has the following general form,

$$G(x, u, \mathbf{s}) = \exp\left\{-x^2 / 2\mathbf{s}^2\right\} \cos(2\mathbf{p}ux) , \quad (1)$$

where u is the frequency of the sinusoidal wave and \mathbf{s} is the standard derivation of the Gaussian envelope. The resultant values are small when a separable eyelash convolutes with the filter. In fact, the filter serves as an edge detector. If a resultant value of a point is smaller than a threshold, it is noted that this point belongs to an eyelash. Mathematically, it can be represented by

$$f(x) * G(v, u, \mathbf{s}) < K_1 , \quad (2)$$

where K_1 is a pre-defined threshold that is -45 using in the following experiments and “*” represents an operator of convolution.

2.2. Multiple Eyelash

For multiple eyelashes, many eyelashes overlap in a small area, which results in less intensity variation in this area. Thus, for detecting multiple eyelashes, if the variance of intensity in the area is less than a threshold, the center of the window is noted as a pixel of eyelash. It can be described by,

$$\frac{\sum_{i=-N}^N \sum_{j=-N}^N (f(x+i, y+j) - M)^2}{(2N+1)^2} < K_2, \quad (3)$$

where M is the mean of intensity in the small window; $(2N+1)^2$ is the window size and K_2 is a threshold. In the following experiments, K_2 is defined as 6 and $(2N+1)^2$ as 5×5 .

2.3. Connective Property

In order to provide more robust and accurate detection method, the connective property of an eyelash is utilized to avoid misclassification from the previous inequalities, Eqs. 2-3. Each point in an eyelash should connect to another eyelash point or to an eyelid. If any point fulfills one of the two previous inequalities, its neighbor pixels are required to check whether they belong to an eyelash or eyelid. If none of the neighbor pixels has been classified as a point in an eyelid or an eyelash, it does not be classified as a pixel in an eyelash.

3. Reflection Detection

Similar to eyelash detection model, reflection is also classified into two classes, strong and weak (see Fig. 2). For a pixel of strong reflection, its intensity should be larger than a certain threshold. Weak reflection is a transition region between strong reflection and the iris. Based on the definition of strong reflection, it can be recognized by a simple inequality, $f(x,y) > K_3$, where K_3 is a threshold, which is taken as 180, used in the following experiments.

According to our discovery, the intensity of the iris pixels closes to a normal distribution. 50 iris images are selected to prove this statement, as shown in Fig. 4, where the black and gray lines are represented as a standard normal cumulative distribution and an empirical cumulative distribution, respectively. The empirical cumulative distribution is generated by the normalized intensity pixels, which are computed by the following equation,

$$d(x, y) = \frac{f(x, y) - \bar{x}}{S}, \quad (4)$$

where \bar{x} and S are the sample mean and sample standard derivation of an iris intensity, respectively.

This discovery motivates us to apply a statistical test to determining weak reflection pixels. This test bases on the following equation,

$$\boldsymbol{m} + \boldsymbol{a}\boldsymbol{s} < f(x, y), \quad (5)$$

where μ and \boldsymbol{s} are mean and standard deviation of the intensity distribution of the iris pixel, respectively; \boldsymbol{a} is a parameter that controls false acceptance and false rejection rates. Based on the Eq. 5, we need to estimate μ and \boldsymbol{s} by sample mean, \bar{X} and sample standard deviation S , respectively. They can be obtained by the following equations,

$$\bar{X} = \frac{\sum_{(x,y) \in P} f(x, y)}{N_p}, \quad (6)$$

$$S = \sqrt{\frac{\sum_{(x,y) \in P} f(x, y)^2 - N_p \bar{X}^2}{N_p - 1}}, \quad (7)$$

where P represents a set of pixels that belongs to the iris and N_p is number of pixels in P . The original goal of this paper is to segment the iris pixels from an image; in other word, the iris

pixels are the pixels in P . Our formulation forms a close loop that can be solved by an iterative approach. The steps can be briefly described as below:

- 1) Set $P=P_j$ and $j=0$. P_j is a set of pixels, which does not belong to eyelashes, strong reflection and the eyelids. Compute $\overline{x_j}$ and S_j by Eqs. 6 and 7, respectively. Also count the number of pixels, N_j in P_j . Let Q_j be a set of pixels that belongs to strong reflection.
- 2) According to Eq. 5, test all pixels in P_j , which connect to any pixel in Q_j . If a pixel with intensity x satisfies Eq. 5, it is removed from P_j and inserted into Q_j . Update $\overline{x_j}$, S_j and N_j by the following equations,

$$N_{jnew}=N_j-I, \quad (8)$$

$$\overline{X}_{jnew} = \frac{N_j \overline{X}_j - x}{N_{jnew}}, \quad (9)$$

$$S_{jnew}^2 = \frac{N_{jnew} (S_j^2 - \overline{X}_{jnew}^2) + N_j \overline{X}_j^2 - x^2}{N_{jnew} - 1}, \quad (10)$$

- 3) If none of pixels is removed from P_j in Step 2, set $P=P_j$ and exit. Otherwise, repeat Step 2.

4. Wavelet-Based Iris Recognition Approach

In this section, we modify Boles' recognition method [1] to develop a new iris recognition method for testing our proposed segmentation method. Our iris recognition method is divided into five parts, which are briefly described below.

- 1) **Segmentation:** Apply curve fitting technique to detect inner and outer boundaries of the iris and upper and lower eyelids. Then, implement the proposed noise detection method to segment the eyelashes and reflection.

- 2) **Normalization:** The segmented region is decomposed into eight rings, which are illustrated in Fig. 5. Each ring is transformed to a 1-D signal with fixed length.
- 3) **Wavelet-Based Feature Extraction:** Using Boles idea, 1-D dyadic wavelet is applied to each ring. The original signal is decomposed into several levels as iris features.
- 4) **Matching:** The dissimilarity between two iris features is measured by l_1 norm.

5. Experimental Results

Many different iris images have been selected to test the proposed segmentation method. Fig. 6 shows some examples. The inner and outer boundaries of the irises and the upper and lower boundaries of eyelids of Fig. 6 are detected by [5]. The white regions of Figs. 6(c) and (d) illustrate the eyelashes and reflection detected by the proposed method. A lot of eyelashes and reflection still remain in the segmented areas of Figs. 6(a) and (b). However, Figs. 6(c) and (d) show that many of them are detected by the proposed method.

In the following experiment, we use the iris recognition approach described in Section 4 to investigate the effectiveness of the proposed segmentation method for iris recognition. Our testing database has 238 images from 48 irises. All the irises are lighted up by infrared light and captured by a CCD camera. In the experiment, four different wavelets, Haar, Gabor, Shannon and Mexican hat, are tested under several sets of parameters. Their formulas are shown below:

Normalized Mexican hat:

$$w_M(t, \mathbf{s}) = \frac{2}{p^{1/4} \sqrt{3\mathbf{s}}} \left(\frac{t^2}{\mathbf{s}^2} - 1 \right) \exp\left(-\frac{t^2}{2\mathbf{s}^2} \right), \quad (11)$$

Shannon:

$$w_s(t) = \frac{\sin(2\mathbf{p}(t - \frac{1}{2}))}{2\mathbf{p}(t - \frac{1}{2})} - \frac{\sin(\mathbf{p}(t - \frac{1}{2}))}{\sin(\mathbf{p}(t - \frac{1}{2}))}, \quad (12)$$

Haar:

$$w_h(t) = \begin{cases} 1 & \text{if } 0 \leq t < 0.5 \\ 2 & \text{if } 0.5 \leq t < 1, \\ 0 & \text{otherwise} \end{cases}, \quad (13)$$

Gabor:

$$w_g(t, \mathbf{s}, \mathbf{h}) = \frac{1}{\sqrt[4]{\mathbf{s}^2 \mathbf{p}}} \exp\left(\frac{-t^2}{2\mathbf{s}^2}\right) \exp(i2\mathbf{p}ht). \quad (14)$$

All the wavelets and their parameters are mentioned in Table 1. The theoretical details of the wavelets and their properties can be referred to [6-7]. The equal error rates of different wavelets at different levels, which prove the usefulness of the proposed segmentation method, show in Table 2, where $Re(w_{gi})$ and $Im(w_{gi})$ represent the real and imaginary parts of the Gabor wavelet using i^{th} set parameters, respectively. For each wavelet at one certain level, two equal error rates are produced. One uses our proposed method and another does not. The numbers in the brackets are the percentage of improvements by our method in term of equal error rates. The equal error rates using our proposed segmentation technique are always smaller than or equal to the corresponding equal error rates without using our model. Some wavelets at some levels are not sensitive to eyelashes and reflection; however, they only provide relatively low recognition rates. As an example, the smallest equal error rate that does not improved by the proposed model is 21%. The smallest equal error rate is 11%, which also gains the greatest improvement (3% equal error rate) from our method.

6. Conclusions

A new eyelash and reflection detection models for accurate iris segmentation has been developed and reported in this paper. A number of images are selected to evaluate the accuracy of the segmentation method and experimental results are encouraging. Based on the modified Boles' recognition engine and using several wavelets with different parameters for testing, the usefulness of our segmentation technique is ensured. According to the experimental results, the proposed method can reduce 3% equal error rate for the iris recognition approach.

Acknowledgments

The work is partially supported with UGC (CRC) fund from the Hong Kong SAR Government and central fund from The Hong Kong Polytechnic University.

References:

1. W.W. Boles and B. Boashash, "A human identification technique using images of the iris and wavelet transform," *IEEE Transactions on Signal Processing*, 46, (1998) 1185-1188.
2. R. Wildes, "Iris Recognition: An emerging biometric technology," *Proceedings of the IEEE*, 85, (1997) 1349-1363.
3. J. Daugman, "High confidence visual recognition of persons by a test of statistical independence," *IEEE Transactions on Pattern Analysis and Machine Intelligence*, 15, (1993) 1148-1161.
4. J. Colton, *Iridology: health analysis and treatments from the iris of the eye*. Queensland, Element, 1996.
5. Y. Zhu, T. Tan and Y. Wang, "Biometric personal identification based on iris pattern," *Proceedings of the 15th International Conference on Pattern Recognition*, 2, (2000) 801-804.
6. G. String and T. Nguyen, *Wavelets and Filter Banks*, Wellesley- Cambridge Press, 1997.
7. S. Mallat, *A wavelet tour of signal processing*, Academic Press, 1998.
8. R.C. Gonzales and R.E. Woods, *Digital Image Processing*, Addison-Wesley Publishing Company. Inc, 1993.
9. A.K. Jain, *Fundamentals of Digital Image Processing*, Prentice Hall, 1989.

Figures:

- Fig. 1. A result of previous iris segmentation approaches.
- Fig. 2. Two types of eyelashes and reflection are defined in an iris image.
- Fig. 3. Cross section of a separable eyelash gray level.
- Fig. 4. Comparison between cumulative distribution of a normal distribution and a cumulative distribution of intensity of an iris image. The gray and black curves represent the normal and iris distribution respectively. Their means and standard deviations are same.
- Fig. 5. Illustration of decomposed regions for feature extraction.
- Fig. 6. Different segmented results from previous iris segmentation approaches with and without the proposed method, (a) and (b) Result from previous approaches, (b) and (d) Result the using the proposed method.

Tables:

- Table 1. Different wavelets and parameters using in the experiments.
- Table 2. The equal error rates are produced by different wavelets at different levels.

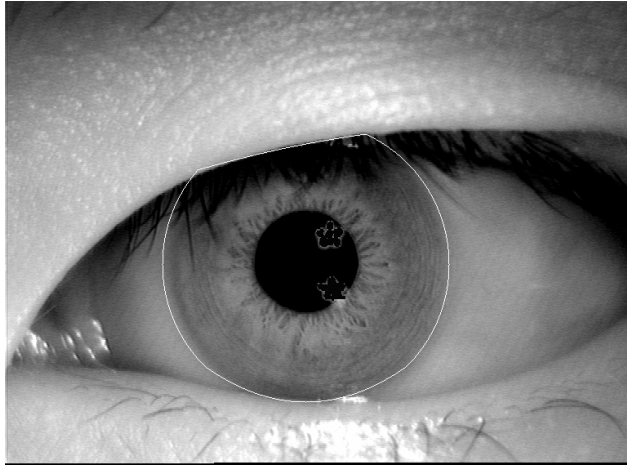


Fig. 1

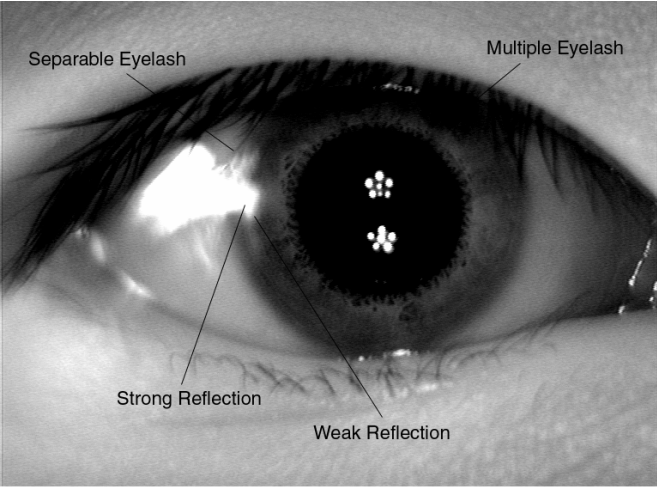


Fig. 2

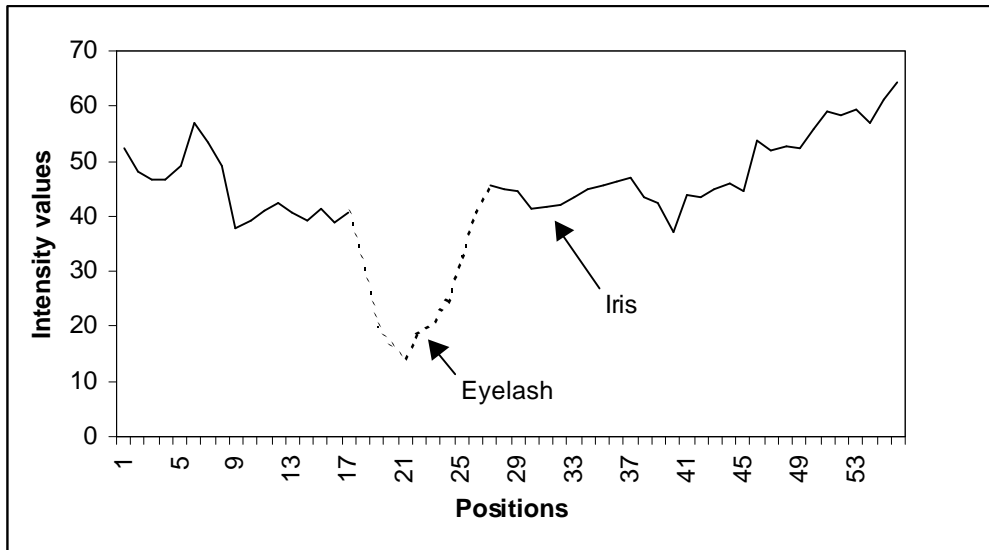


Fig. 3

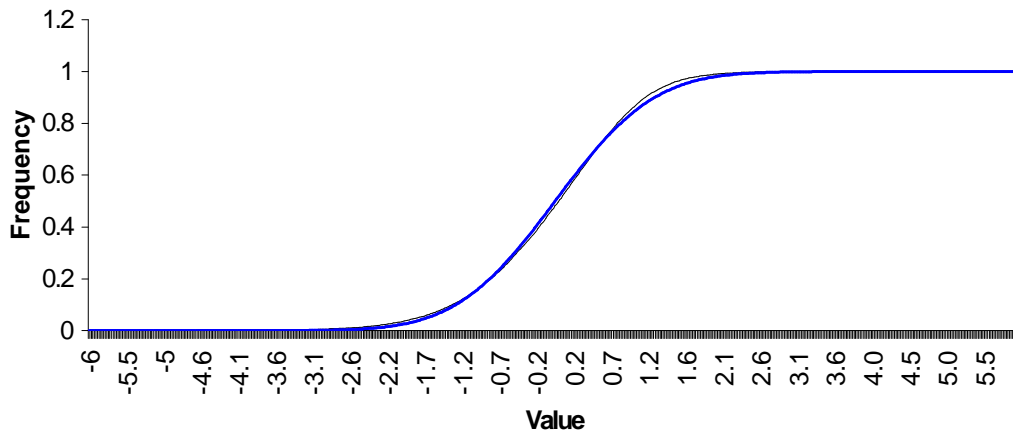


Fig. 4

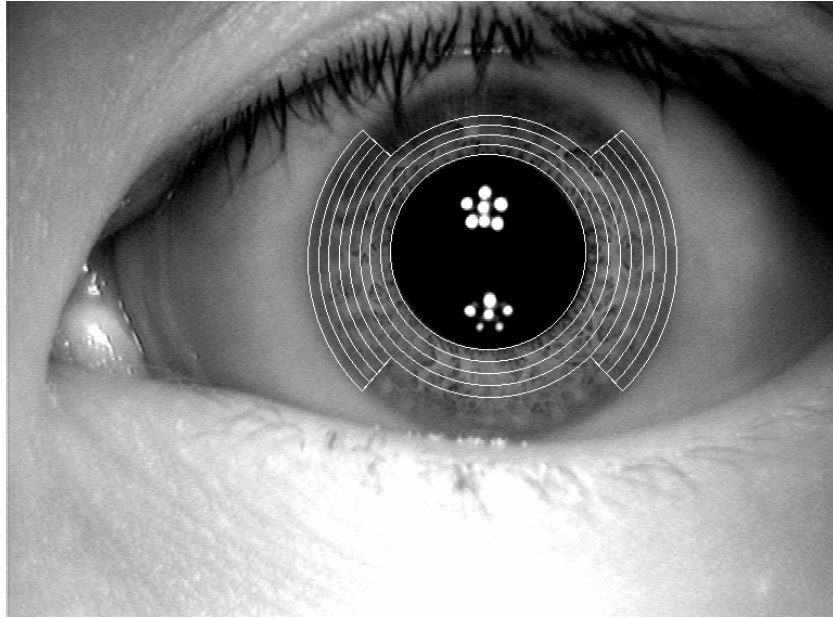
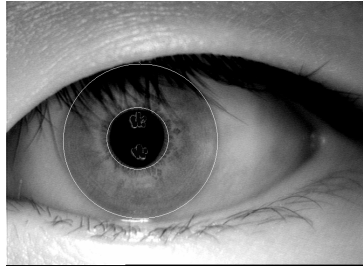
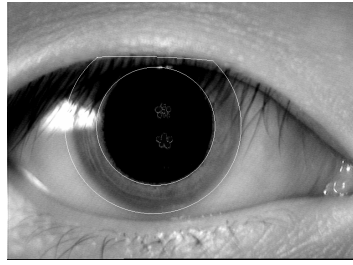


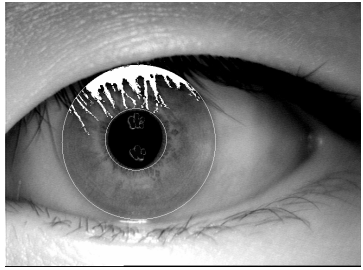
Fig. 5



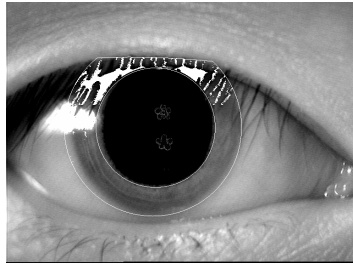
(a)



(b)



(c)



(d)

Fig. 6

Tables:

Table 1

Symbol	Wavelets	Parameters
w_{M1}	Mexican Hat	$w_M(x, 0.2), \mathbf{s}=0.2$
w_{M2}	Mexican Hat	$w_M(x, 0.3), \mathbf{s}=0.3$
w_{M3}	Mexican Hat	$w_M(x, 0.4), \mathbf{s}=0.4$
w_{M4}	Mexican Hat	$w_M(x, 0.75), \mathbf{s}=0.75$
w_{M5}	Mexican Hat	$w_M(x, 2), \mathbf{s}=2.0$
w_h	Haar Wavelet	$w_h(x)$
w_s	Shannon	$w_s(x)$
w_{g1}	Gabor	$w_g(x, 0.3512, 1.4663), \mathbf{s}=0.3512, \mathbf{h}=1.4663$
w_{g2}	Gabor	$w_g(x, 0.7023, 0.7332), \mathbf{s}=0.7023, \mathbf{h}=0.7332$
w_{g3}	Gabor	$w_g(x, 1.4046, 0.3666), \mathbf{s}=1.4046, \mathbf{h}=0.3666$

Table 2

Wavelets	Equal Error Rate (%)							
	Level 1		Level 2		Level 3		Level 4	
	Without Model	Using Model	Without Model	Using Model	Without Model	Using Model	Without Model	Using Model
w_{M1}	23	23 (0)	22	22 (0)	30	29 (1)	21	19 (2)
w_{M2}	23	23 (0)	31	31 (0)	24	22 (2)	16	13 (3)
w_{M3}	22	22 (0)	30	29 (1)	21	19 (2)	18	16 (2)
w_{M4}	31	30 (1)	22	20 (2)	16	14 (2)	24	24 (0)
w_{M5}	18	16 (2)	21	21 (0)	24	24 (0)	24	24 (0)
w_h	28	27 (1)	21	21 (0)	19	18 (1)	15	12 (3)
w_s	23	23 (0)	23	23 (0)	23	23 (0)	23	23 (0)
$Re(w_{g1})$	23	23 (0)	23	23 (0)	36	34 (2)	24	23 (1)
$Re(w_{g2})$	23	23 (0)	36	34 (2)	24	23 (1)	18	16 (2)
$Re(w_{g3})$	36	34 (2)	24	23 (1)	18	16 (2)	23	23 (0)
$Im(w_{g1})$	21	20 (1)	21	20 (1)	35	34 (1)	26	24 (2)
$Im(w_{g2})$	21	20 (1)	35	34 (1)	26	24 (2)	14	11 (3)
$Im(w_{g3})$	35	34 (1)	26	24 (2)	14	11 (3)	13	11 (2)